

See discussions, stats, and author profiles for this publication at: <https://www.researchgate.net/publication/232417011>

CO₂ Capturing Mechanism in Aqueous Ammonia: NH₃-Driven Decomposition-Recombination Pathway

ARTICLE in JOURNAL OF PHYSICAL CHEMISTRY LETTERS · APRIL 2011

Impact Factor: 7.46 · DOI: 10.1021/jz200095j

CITATIONS

23

READS

105

8 AUTHORS, INCLUDING:



Dongyoung Kim

Samsung Advanced Institute of Technology

19 PUBLICATIONS 617 CITATIONS

SEE PROFILE



Yeonchoo Cho

Pohang University of Science and Technology

16 PUBLICATIONS 511 CITATIONS

SEE PROFILE



Kunwoo Han

Research Institute of Industrial Science and ...

22 PUBLICATIONS 198 CITATIONS

SEE PROFILE



Kwang-Sun Kim

Korea University of Technology and Education

554 PUBLICATIONS 30,560 CITATIONS

SEE PROFILE

CO₂ Capturing Mechanism in Aqueous Ammonia: NH₃-Driven Decomposition–Recombination Pathway

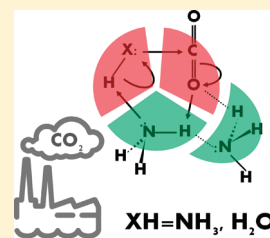
Dong Young Kim,[†] Han Myoung Lee,[†] Seung Kyu Min,[†] Yeonchoo Cho,[†] In-Chul Hwang,[†] Kunwoo Han,[‡] Je Young Kim,[‡] and Kwang S. Kim^{*,†}

[†]Center for Superfunctional Materials, Department of Chemistry, Pohang University of Science and Technology, San 31, Hyojadong, Pohang 790-784, Republic of Korea

[‡]CO₂ Project, Research Institute of Industrial Science & Technology, San 32 Hyojadong, Pohang 790-600, Republic of Korea

 Supporting Information

ABSTRACT: Capturing CO₂ by aqueous ammonia has recently received much attention due to its advantages over other state-of-the-art CO₂-capture technology. Thus, understanding this CO₂-capturing mechanism, which has been causing controversy, is crucial for further development toward advanced CO₂ capture. The CO₂ conversion mechanism in aqueous ammonia is investigated using ab initio calculations and kinetic simulations. We show full details of all reaction pathways for the NH₃-driven conversion mechanism of CO₂ with the pronounced effect of microsolvation. Ammonia performs multiple roles as reactant, catalyst, base, and product controller. Both carbamic and carbonic acids are formed by the ammonia-driven trimolecular mechanism. Ammonia in microsolvation makes the formation of carbamic acid kinetically preferred over carbonic acid. As the concentration of CO₂ increases, the dominant product becomes carbonic acid. The conversion from carbamic acid into carbonic acid occurs through the decomposition–recombination pathway. This understanding would be exploited for the optimal CO₂ capture technology.



SECTION: Energy Conversion and Storage

Despite numerous debates it is widely accepted that the accumulation of greenhouse gases in the atmosphere causes an enhanced greenhouse effect, leading to climate change and global warming.^{1,2} Hence, there is major scientific interest in preventing the release of CO₂ and lowering its concentration in the atmosphere. The development of technologies such as capturing and storing CO₂ for various commercial applications^{3–7} provides a midterm solution to reduce environmental problems, allowing us to use carbon-based fuels until an alternative new energy source matures.^{8–12} Currently, the amine scrubbing process is the leading technology for CO₂ capture, and this process is predicted to be the dominant technology for CO₂ capture from coal-fired power plants in 2030.^{13,14} An alternative advanced technique, capturing CO₂ by aqueous ammonia (Scheme 1),^{15–18} has recently received much attention due to its advantages over the conventional amine-based technique. However, few reports dealing with the ammonia process are available. Although there are papers that demonstrate the CO₂ conversion mechanism in the pure aqueous system,^{19,20} there is no clear understanding of the reaction mechanism of CO₂ in aqueous ammonia solutions, while there are some incorrect speculations on this reaction mechanism. There is thus an urgency to detail the conversion mechanism of CO₂ in aqueous ammonia, with this study being the first to elucidate details of the mechanism. In both fundamental and applied points of view, this study provides important information about CO₂ capture for future green chemistry.

CO₂ in the aqueous phase exists almost entirely in the form of hydrated CO₂ and 1% H₂CO₃.¹⁹ However, in the case of CO₂ in aqueous ammonia solutions, it exists primarily as a converted

form of NH₂COOH or H₂CO₃, with these molecules primarily in ionic forms due to their acid–base behavior, with the dominant product depending on the ratio of reactants.¹⁸ When the amounts of CO₂ and NH₃ are comparable, H₂CO₃ is the main product in solution; however, when an excess of NH₃ exists, NH₂COOH becomes the main product in solution.

For the formation of carbamates, originally, a two-step zwitterion mechanism had been suggested.^{21,22} However, this mechanism was proved to be unlikely, and rather, a synchronous trimolecular mechanism was proposed.²³ When CO₂ reacts with NH₃ to form a carbamate in the aqueous phase, the bond formation between the C in CO₂ and the N in NH₃ takes place simultaneously with a proton transfer to a nearby base (B), CO₂ + NH₃ + B ↔ NH₂COO[–] + BH⁺. However, the previous investigations have been limited only to the formation of the carbamate species.^{23–25} The function of the catalytic base is important, but its understanding remains uncertain. The role of microsolvation around the reaction core has never been considered in the past studies. The details of the reaction mechanism for CO₂ in aqueous ammonia, being dynamically controlled by the ratio of reactants, are not clearly understood. In this regard, we try to shed light on the comprehensive reaction mechanism of CO₂ in aqueous ammonia, using ab initio calculations and kinetic simulations. Finally, the NH₃-driven catalytic conversion processes of CO₂ with an effective perturbation by microsolvation are shown in full detail for all reaction pathways, which include the

Received: January 20, 2011

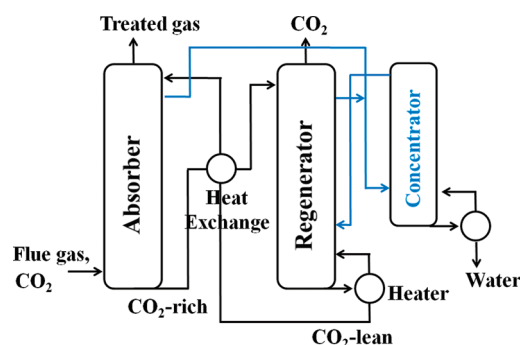
Accepted: March 1, 2011

Published: March 07, 2011

conversion processes of CO₂ into either carbamic or carbonic acids and between carbamic and carbonic acids.

To properly model the nanoscopic nature of the reaction region of CO₂ in aqueous ammonia, we investigate the potential energy surfaces of reaction pathways from the decomposed combination of CO₂, NH₃, and H₂O to either NH₂COOH or H₂CO₃ with a varying number of active solvent molecules and with the change in molar ratio of NH₃/H₂O. Then, the catalytic efficiencies are compared. In bulk, the decomposed reactants exist primarily in molecular forms, while the products, NH₂COOH or H₂CO₃, are primarily in ionic forms due to their

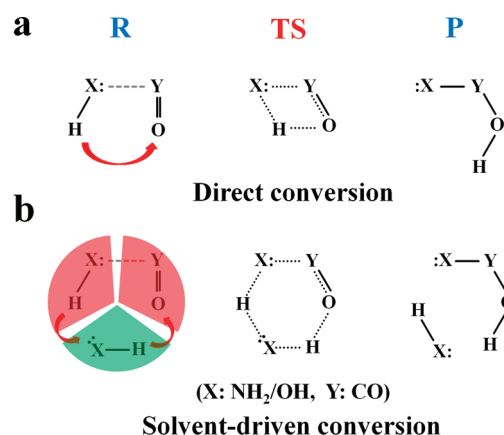
Scheme 1. Schematic Flow Diagram of the POSCO/RIST Pilot Plant for CO₂ Capture Using Aqueous Ammonia^a



^a Flue gas containing CO₂ enters into the absorber. Aqueous ammonia selectively absorbs CO₂ and forms a CO₂-rich solution. The solution is then pumped to the regenerator and heated up to form pure CO₂. As a result, the pure CO₂ is released at the top of the regenerator. The CO₂-lean solution is recycled back to the absorber and reused. The concentrator is used for the ammonia vapor recovery. The POSCO/RIST Pilot Plant can treat flue gas at a rate of 1000 N m³/h, producing 3000 tons of CO₂ annually (see Supporting Information).

acid–base behavior. At the initial stage of the CO₂ conversion process, the reaction is like a gas-phase one at the interface between gas and solution because CO₂ is hardly soluble at the moment that the solution is spread over CO₂; thus, the transition state is also almost the gas-like state. Moreover, at the final stage of the reaction after passing the transition barrier, the product is much more stable than the reactant in solution. Thus, this CO₂ conversion takes place by overcoming an early transition state, which then should be similar to the gas-phase transition state. Therefore, our model calculation with molecular clusters successfully depicts the reactant mechanism in bulk systems. Figure S1 in Supporting Information and Figures 1 and 2 show the potential energy surface of the reactions, $\text{H}_2\text{CO}_3 + (m - n - 1)\text{H}_2\text{O} + n\text{NH}_3 \leftrightarrow \text{CO}_2 + (m - n)\text{H}_2\text{O} + n\text{NH}_3 \leftrightarrow$

Scheme 2. Schematic Views of Direct and Solvent-Driven Conversions into H₂CO₃ and NH₂COOH (P) from the Decomposed Reactants (R)^a



^a TS: transition state; X = NH₂/OH and Y = CO.

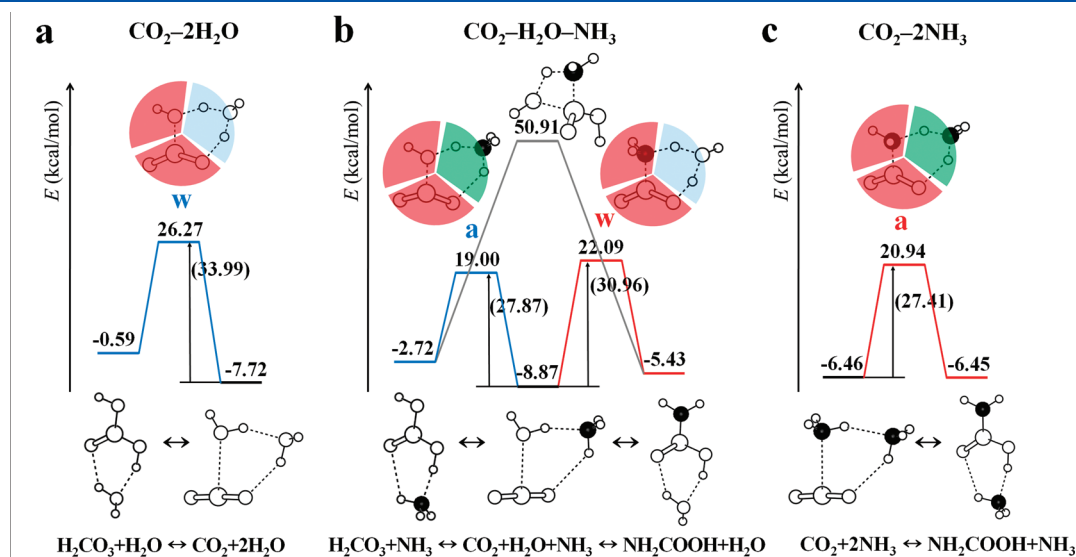


Figure 1. Potential energy surfaces of the reaction pathways for conversions between the decomposed reactants and the acidic products H₂CO₃ and NH₂COOH in complexes CO₂-(2-n)H₂O-nNH₃. The ratio of NH₃/H₂O is changed (n = 0–2 in a–c). The reactions occur along the single water or ammonia catalytic pathways (w or a). The energies along the pathways are obtained from CCSD(T)/aug-cc-pVDZ//MP2/aug-cc-pVDZ//MP2/aug-cc-pVDZ relative to the decomposed reactants (Supporting Information). Conversion into H₂CO₃ is represented by the blue line, and conversion into NH₂COOH is presented by the red line. The one-step exchange pathway between H₂CO₃ and NH₂COOH is represented by the gray line. A N atom is given in black, H by a small circle, O by a medium circle, and C by a large circle.

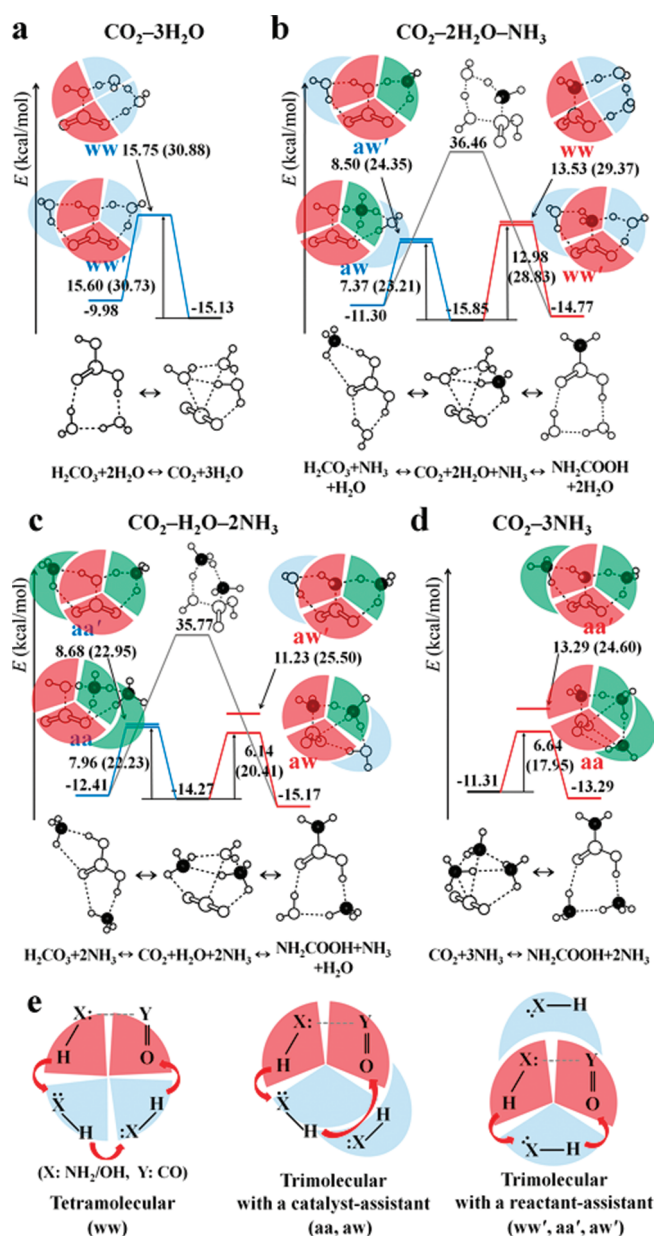


Figure 2. Potential energy surfaces of the reaction pathways for conversions between the decomposed reactants and the acidic products H_2CO_3 and NH_2COOH in complexes $\text{CO}_2\text{--}(3-n)\text{H}_2\text{O--}n\text{NH}_3$. The ratio of $\text{NH}_3/\text{H}_2\text{O}$ ($n = 0\text{--}3$) changes in (a–d). The reactions occur along the double water/water, ammonia/water, or ammonia/ammonia catalytic pathways (ww/ww', aw/aw', or aa/aa'). The ww-type reaction occurs via a single-step tetramolecular mechanism, the aa- and aw-type reactions occur via a trimolecular mechanism with a catalyst assistant, and ww'-, aa'-, and aw'-type reactions occur via a trimolecular mechanism with a reactant assistant. Schematic views of these mechanisms are shown in (e). The relative energies are obtained from CCSD(T)/aug-cc-pVDZ//MP2/aug-cc-pVDZ//MP2/aug-cc-pVDZ. Conversion into H_2CO_3 is represented by a blue line, and conversion into NH_2COOH is presented by a red line. The one-step exchange pathway between H_2CO_3 and NH_2COOH is represented by a gray line. A N atom is given in black, H by a small circle, O by a medium circle, and C by a large circle.

$\text{NH}_2\text{COOH} + (m-n)\text{H}_2\text{O} + (n-1)\text{NH}_3$ ($n = 0\text{--}m$, where $m = 1\text{--}3$). The trends of activation energy (E_a) and reaction energy (ΔE) are presented in Figure 3. For each barrier on the reaction

pathway, the microcanonical rate constant is obtained using Rice–Ramsperger–Kassel–Marcus (RRKM) theory,²⁶ with the microcanonical rate constant obtained being converted to the thermal rate constant (k). Tunnelling corrections are included by utilizing the Skodje and Truhlar approximations.²⁷

Extremely Rare Direct Conversion. In $\text{CO}_2\text{--}(1-n)\text{H}_2\text{O--}n\text{NH}_3$ ($n = 0\text{--}1$), the conversion from $\text{CO}_2 + \text{NH}_3/\text{CO}_2 + \text{H}_2\text{O}$ to $\text{NH}_2\text{COOH}/\text{H}_2\text{CO}_3$ is a reversible process, as shown in Figure S1 (Supporting Information). Initially, the reactant $\text{CO}_2 + \text{NH}_3/\text{CO}_2 + \text{H}_2\text{O}$ is characterized by the interaction between $\text{C}^{\delta+}$ in CO_2 and $\text{N}^{\delta-}/\text{O}^{\delta-}$ in $\text{NH}_3/\text{H}_2\text{O}$. In the conversion to $\text{NH}_2\text{COOH}/\text{H}_2\text{CO}_3$, $\text{CO}_2 + \text{NH}_3/\text{CO}_2 + \text{H}_2\text{O}$ forms a C–N/O bond with a simultaneous proton crossing into an electron-rich O site in CO_2 . However, without a catalyst, the ring strain of the transition state leads to quite a high energy barrier. The E_a 's of the $\text{CO}_2 + \text{NH}_3 \rightarrow \text{NH}_2\text{COOH}$ and $\text{CO}_2 + \text{H}_2\text{O} \rightarrow \text{H}_2\text{CO}_3$ reactions are 51.7 and 47.2 kcal/mol, respectively. The k 's at 300 K are 3×10^{-18} and $3 \times 10^{-21} \text{ s}^{-1}$, respectively, indicating that these direct (d) conversion processes are extremely rare events. As illustrated in Scheme 2, the conversion process of CO_2 into either NH_2COOH or H_2CO_3 in an aqueous ammonia solution happens via the catalytic effect of solvent molecules.

Catalytic Base NH_3 . The activation energy barrier for the reaction of CO_2 with $\text{H}_2\text{O}/\text{NH}_3$ drastically decreases with the inclusion of a single catalytic H_2O (w) or NH_3 (a) to the complexes of $\text{CO}_2\text{--}(2-n)\text{H}_2\text{O--}n\text{NH}_3$ ($n = 0\text{--}2$) (Figures 1 and 3). The catalytic solvent molecule acts as a proton shuttle, thereby forming a no-strain trimolecular transition state. Due to the higher basicity of NH_3 over H_2O , the a-type pathway has a lower energy barrier than the w-type pathway. An inclusion of one NH_3 molecule to the reactions $\text{H}_2\text{O} + \text{CO}_2 \rightarrow \text{H}_2\text{CO}_3$ and $\text{NH}_3 + \text{CO}_2 \rightarrow \text{NH}_2\text{COOH}$ yields E_a 's of 27.9 and 27.4 kcal/mol, respectively. The energy barriers for the two reactions are lower than the d pathway by 23.8 (46%) and 19.8 kcal/mol (42%) respectively, while the rates are faster by a factor of 10^{11} and 10^7 at 300 K, respectively. The inclusion of one H_2O molecule reduces the energy barriers for the reactions by 34%. The conversion of hydrated CO_2 into H_2CO_3 occurs by the catalysis of water molecules in the aqueous phase.^{19,20} However, in the case of the reaction of CO_2 in aqueous ammonia, the NH_3 -driven pathway is favored.

Pronounced Effect of Microsolvation on the Formation of NH_2COOH . The effects of the inclusion of two active solvent molecules are investigated on the $\text{CO}_2\text{--}(3-n)\text{H}_2\text{O--}n\text{NH}_3$ ($n = 0\text{--}3$) complexes in Figures 2 and 3. The first solvent molecule acts as a proton shuttle, forming a trimolecular reaction. With the introduction of the second solvent molecule, two different types of reaction channels compete with each other.²⁰ First, the trimolecular reaction is aided by the second solvent molecule near the site of the proton transfer. Thus, depending on the ratio of $\text{NH}_3/\text{H}_2\text{O}$, three different types of H-bonded solvent networks are formed, (i) $\text{H}^+ \cdots \text{H}_2\text{O} \cdots \text{H}_2\text{O} \cdots \text{O}^-$ (ww), (ii) $\text{H}^+ \cdots \text{NH}_3 \cdots \text{H}_2\text{O} \cdots \text{O}^-$ (aw), and (iii) $\text{H}^+ \cdots \text{NH}_3 \cdots \text{NH}_3 \cdots \text{O}^-$ (aa). Second, the trimolecular reaction is aided by the second solvent molecule, denoted by a prime ('), on the opposite side to the site of the proton transfer forming two fused-trimeric ring structures, (iv) $\text{H}_2\text{O} \cdots \text{XH}^+ \cdots \text{H}_2\text{O} \cdots \text{O}^-$ (ww'), (v) $\text{H}_2\text{O} \cdots \text{XH}^+ \cdots \text{NH}_3 \cdots \text{O}^-$ (aw'), and (vi) $\text{NH}_3 \cdots \text{XH}^+ \cdots \text{NH}_3 \cdots \text{O}^-$ (aa'), where $\text{X} = \text{NH}_2/\text{OH}$. The second active solvent molecule can assist the reaction either as a direct participant forming a tetramolecular intermediate or as a spectator molecule around the reaction core.

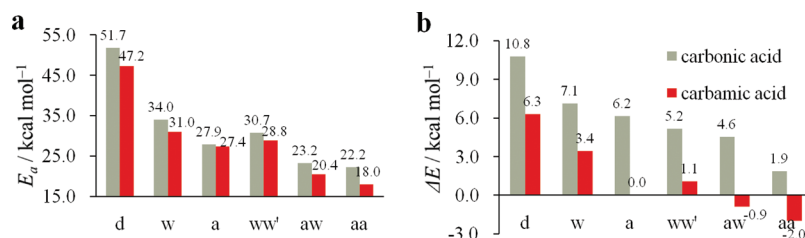


Figure 3. Activation energies (E_a) and reaction energies (ΔE) obtained from the CCSD(T)/aug-cc-pVDZ//MP2/aug-cc-pVDZ//MP2/aug-cc-pVDZ level of theory for H_2CO_3 and NH_2COOH formation by the direct pathway (d), the one catalytically active solvent molecule pathway (w, H_2O ; a, NH_3), and the two catalytically active molecule pathways (ww', $2\text{H}_2\text{O}$; aw, $\text{NH}_3-\text{H}_2\text{O}$; aa, 2NH_3).

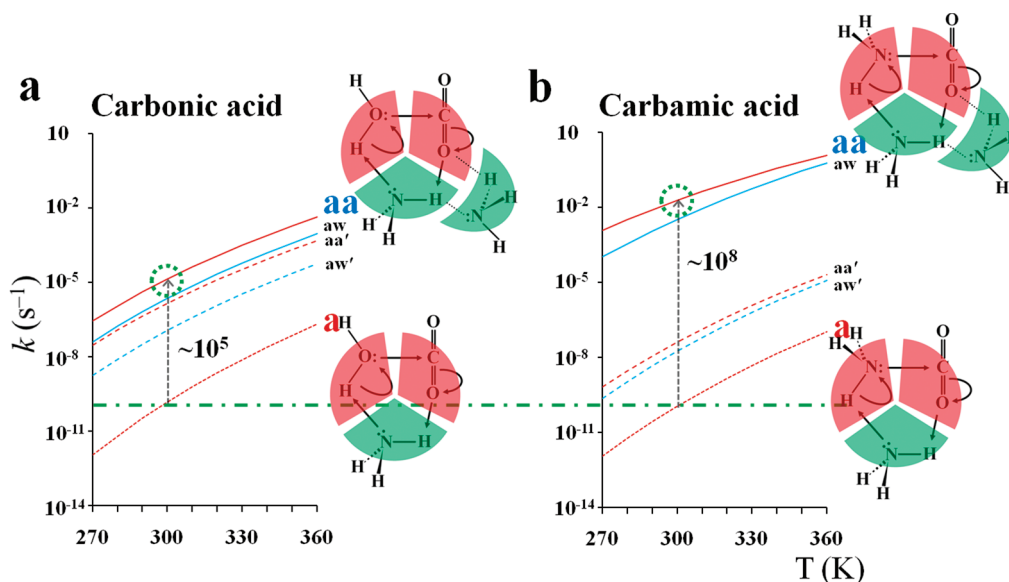


Figure 4. Rate constants for the formation of H_2CO_3 (a) and NH_2COOH (b) from the decomposed reactants. The aa-type pathway is dominant for both reactions. Along the a-type pathway, the formations of H_2CO_3 and NH_2COOH have similar reaction rates. Along the aa-type pathway, the formation of NH_2COOH becomes kinetically ~ 3 orders faster in magnitude than the formation of H_2CO_3 . The contribution ratio of each aa/aw/aa'/aw' pathway ($k_{aa}/k_{aw}/k_{aa'}/k_{aw'}$ at 300 K) is 1:0.2:0.1:0.01 for the formation of H_2CO_3 , while the contribution ratio of each aa/aw pathways (k_{aa}/k_{aw} at 300 K) is 1:0.2 for the formation of NH_2COOH , with the contributions of the aa' and aw' pathways being insignificant. These indicate that the catalytic effects of ammonia and water molecules in the first solvation shell in the conversion process for the carbonic and carbamic acids are very different from each other.

For the ww-type, triple proton transfer occurs simultaneously via the H-bonding chain of two catalytic H_2O molecules through a synchronous tetramolecular mechanism. However, for the aa- and aw-types, a proton in a transient NH_4^+ moves directly into an O site in CO_2 , thereby not mediating the next NH_3 or H_2O molecule. This means that only the nearest NH_3 molecule participates directly in the proton shuttle reaction. The other NH_3 or H_2O molecule, which is H-bonded to a catalyst, assists the reaction by stabilizing transition states near the catalyst. This demonstrates the a-type trimolecular mechanism with a catalyst assistant. For the ww-, aa-, and aw'-types, only the nearest solvent molecule is directly involved in the proton shuttle reaction, in a way similar to that seen for aa- and aw-types. The other solvent molecule stabilizes the transition state on the opposite side of the proton transfer by being H-bonded to a reactant. This shows a trimolecular mechanism with a reactant assistant. Schematic illustrations of these mechanisms are presented in Figure 2e.

Among various pathways, the aa-type shows the lowest-energy pathway and the most accelerated rate constant. The E_a 's of the aa-type pathway for the formation of H_2CO_3 and NH_2COOH are 22.2 and 17.9 kcal/mol, respectively; the k 's at 300 K are 1×10^{-5}

and $2 \times 10^{-2} \text{ s}^{-1}$, respectively, showing an increase of a factor of $\sim 10^5$ and $\sim 10^8$ compared to the a pathway (Figure 4). This illustrates that microsolvation of the reaction core by NH_3 molecules effectively aids the a-type trimolecular reaction. By neglecting solvation, the NH_2COOH and H_2CO_3 formations show nearly isoenergetic activation barriers and similar reaction rates along the a pathway. Due to the substantial effect of microsolvation on the formation of NH_2COOH compared to that of H_2CO_3 , the formation of NH_2COOH becomes kinetically faster than that of H_2CO_3 .

Also, we should note that the aw-, aa'-, and aw'-types contribute to the conversion reaction into H_2CO_3 with $k_{aa}/k_{aw}/k_{aa'}/k_{aw'} = 1:0.2:0.1:0.01$ at 300 K. The aw, aa', and aw' pathways which form H_2CO_3 require $\sim 1\text{--}2$ kcal/mol higher activation energies than the aa pathway. On the other hand, only the aw pathway contributes to the conversion reaction into NH_2COOH ($k_{aa}/k_{aw} = 1:0.2$ at 300 K), while the contributions of the aa' and aw' pathways are insignificant. The aa' and aw' pathways which form NH_2COOH require $\sim 6\text{--}7$ kcal/mol higher energies than the aa pathway. In the case of H_2CO_3 , the effect of microsolvating the trimolecular reaction both near the site and on the opposite side of the proton transfer are important. However, in the case of NH_2COOH , microsolvating the trimolecular reaction near the site

of the proton transfer aids the reaction more effectively than that on the opposite side of the proton transfer.

Applying implicit solvents utilizing the self-consistent reaction field (SCRF) theory with the isodensity surface polarized continuum model (IPCM),²⁸ polar transition states are more stabilized, which leads to the lowering of the E_a 's by ~ 11 kcal/mol. This results in an enhancement of k 's by an order of ~ 8 in magnitude, where the $k_{aa+IPCM}$'s toward H_2CO_3 and NH_2COOH become $\sim 10^3$ and $\sim 10^6$ s $^{-1}$, respectively. As the $k_{aa+IPCM}$ is the reaction rate in a unimolecular process, an overall reaction rate constant ($k_{overall}$) is obtained by multiplying the $k_{aa+IPCM}$ by the probability of the formation of an aa cluster in solution ($P_{aa} \approx 10^{-2}$, Supporting Information). Then, the $k_{overall}$'s for H_2CO_3 and NH_2COOH are ~ 10 and $\sim 10^4$ s $^{-1}$, respectively. These results are in good agreement with the experimental rate constants for the reaction of CO_2 in aqueous ammonia solutions ($\sim 10^3$ s $^{-1}$).²⁹ So far, no experimental comparison of kinetic rates between the formation of NH_2COOH and H_2CO_3 from the decomposed reactants has been made. From our calculations, we have shown that the formation of NH_2COOH is kinetically faster than that of H_2CO_3 due to a more pronounced effect of microsolvation.

From NH_2COOH to H_2CO_3 via the Decomposition–Recombination Pathway. While only a small fraction of hydrated CO_2 converts into H_2CO_3 (K_{eq} at 300 K = $\sim 10^{-3}$) in the aqueous phase, the majority of CO_2 converts into NH_2COOH or H_2CO_3 (K_{eq} at 300 K = $\sim 10^3$) in the aqueous ammonia phase. Basic ammonia, which acts as a catalyst in the conversion process, stabilizes the acidic product formed. With the addition of two active H_2O molecules, we observe the decreases of ΔE 's in the formation of NH_2COOH and H_2CO_3 by ~ 5 kcal/mol, while the addition of two active NH_3 molecules leads to the decreases of ΔE 's by ~ 8 – 9 kcal/mol, compared to the d pathway (Figure 3b). Treating the basic bulk implicitly, the SCRF/IPCM calculation for the aa pathway leads to the decreases of ΔE 's by ~ 12 kcal/mol. Then, the $\Delta E_{aa+IPCM}$'s for the formation of NH_2COOH and H_2CO_3 are ~ -6 and ~ -1 kcal/mol, respectively. This shows that the formation of NH_2COOH is both kinetically and energetically favored over that of H_2CO_3 from decomposed reactants.

Thus, when CO_2 enters into aqueous ammonia solutions, carbamic acid is the main species in the initial stage, while it exists primarily in its conjugate form, $NH_3 + NH_3 + CO_2 \rightarrow NH_4^+ + NH_2COO^-$. In this process, one NH_3 molecule acts as a reactant, and the other NH_3 acts as a catalytic base in the trimolecular reaction. NH_3 molecules in the microsolvation shell effectively aid the reaction. When the molar ratio of CO_2 to NH_3 is greater than 1:2, the NH_3 reactant path is blocked, while the energetically favored NH_3 catalytic path is observed. As a result, the formation of bicarbonate species (conjugate form of carbonic acid) starts to accelerate via the reaction $NH_3 + H_2O + CO_2 \rightarrow NH_4^+ + HCO_3^-$, while at the same time, the formation of carbamate species starts to diminish. Thus, one molar equivalent of CO_2 is captured by one molar equivalent of NH_3 instead of two molar equivalents of NH_3 . Regarding the ammonia scrubbing process of CO_2 capture in Scheme 1, the loading of CO_2 into the regenerator in the form of carbonic acid will be more beneficial than the loading in the form of carbamic acid in terms of loading capacity. Also, the less stable C–O bond in carbonic acid requires a lower energy to break than the C–N bond in carbamic acid during the thermal regeneration step.

Transformation from carbamate species to bicarbonate species can occur through two pathways, (i) via the decomposition–

recombination path (red–blue line in Figures 1 and 2) or (ii) via the one-step exchange path (gray line in Figures 1 and 2). In the one-step path, NH_2COOH is transformed into H_2CO_3 through the process where the C in NH_2COOH is attacked by O in H_2O to form a C–O bond with a simultaneous dissociation of a C–N bond, producing NH_3 and H_2CO_3 , with the bound $O \cdots C \cdots N$ structure as the transition state. However, the very high energy barrier of this one-step pathway indicates that the conversion from NH_2COOH to H_2CO_3 takes place through the decomposition–recombination pathway.

In summary, we have detailed the comprehensive reaction mechanism of CO_2 in aqueous ammonia, showing several roles of NH_3 . Regarding the formation of both carbamic and carbonic acids, the H_2O catalytic trimolecular pathway has been considered, while the bases play a certain role. However, we have shown that the reactions take place mainly along the NH_3 catalytic trimolecular pathway. However, via the NH_3 -driven trimolecular reaction in the absence of solvation molecules, the formation of carbamic and carbonic acids requires similar activation energy barriers and reaction rates. Thus, a second active solvent molecule is considered. In our calculation, this solvent molecule does not participate in the proton shuttle reaction directly but instead effectively assists the trimolecular reaction in the microsolvation shell. The differences between the various microsolvation effects in the conversion processes were investigated. We predict that NH_3 molecules in the first microsolvation shell aid the conversion process of carbamic acid more effectively than that of carbonic acid, resulting in the formation of carbamic acid becoming kinetically faster than that of carbonic acid. When the concentration of carbon dioxide is low in aqueous ammonia solutions, the carbamate species is the main product due to its higher stability over the bicarbonate species. In this process, two molar equivalents of ammonia capture one molar equivalent of carbon dioxide, with one ammonia molecule acting as a reactant and the other ammonia molecule acting as a catalytic base. Thus, as the concentration of CO_2 increases, ammonium bicarbonate becomes the dominant species. In this process, one molar equivalent of ammonia captures one molar equivalent of carbon dioxide. The conversion process from carbamate into bicarbonate does not occur through the direct pathway but through the decomposition–recombination pathway. This has never been demonstrated before. This study provides useful information not only for the development of improved CO_2 capture by ammonia or amine scrubbing but also for the design of futuristic techniques for CO_2 capture and utilization.^{7,30,31}

■ ASSOCIATED CONTENT

S Supporting Information. Computational methods, schematic flow diagram of the pilot plant for the CO_2 capture process using aqueous ammonia, and calculated IR Spectra for all transition states and minima. This material is available free of charge via the Internet at <http://pubs.acs.org>.

■ AUTHOR INFORMATION

Corresponding Author

*E-mail: kim@postech.ac.kr.

■ ACKNOWLEDGMENT

This work was supported by KRF (National Honor Scientist Program, WCU: R32-2008-000-10180-0), KISTI (KSC-2008-K08-0002), and RIST (Green Science Program, 2009K053).

■ REFERENCES

- (1) IPCC *Special Report on Carbon Dioxide Capture and Storage*; Cambridge University Press, Cambridge, U.K., 2005.
- (2) Falkowski, P.; et al. The Global Carbon Cycle: A Test of Our Knowledge of Earth as a System. *Science* **2000**, *290*, 291–296.
- (3) Abelson, P. H. Limiting Atmospheric CO₂. *Science* **2000**, *289*, 1293.
- (4) Yang, H.; Xu, Z.; Fan, M.; Gupta, R.; Slimane, R. B.; Bland, A. E.; Wright, I. Progress in Carbon Dioxide Separation and Capture: A Review. *J. Environ. Sci.* **2008**, *20*, 14–27.
- (5) Hunt, A. J.; Sin, E. H. K.; Marriott, R.; Clark, J. H. Generation, Capture, and Utilization of Industrial Carbon Dioxide. *ChemSusChem* **2010**, *3*, 306–322.
- (6) Sakakura, T.; Choi, J.-C.; Yasuda, H. Transformation of Carbon Dioxide. *Chem. Rev.* **2007**, *107*, 2365–2387.
- (7) D'Alessandro, D. M.; Smit, B.; Long, J. R. Carbon Dioxide Capture: Prospects for New Materials. *Angew. Chem., Int. Ed.* **2010**, *49*, 6258–6082.
- (8) Coontz, R.; Hanson, B. Not So Simple. *Science* **2004**, *305*, 957.
- (9) Schlapbach, L. Hydrogen-Fuelled Vehicles. *Nature* **2009**, *460*, 809–811.
- (10) Schlapbach, L.; Züttel, A. Hydrogen-Storage Materials for Mobile Applications. *Nature* **2001**, *414*, 353–358.
- (11) Kim, D. Y.; Singh, N. J.; Lee, H. M.; Kim, K. S. Hydrogen-Release Mechanism in Lithium Amidoboranes. *Chem.—Eur. J.* **2009**, *15*, 5598–5604.
- (12) Kim, D. Y.; Lee, H. M.; Seo, J.; Shin, S. K.; Kim, K. S. Rules and Trends of Metal Cation Driven Hydride-Transfer Mechanisms in Metal Amidoboranes. *Phys. Chem. Chem. Phys.* **2010**, *12*, 5446–5453.
- (13) Rochelle, G. T. Amine Scrubbing for CO₂ Capture. *Science* **2009**, *325*, 1652–1654.
- (14) Puxty, G.; Rowland, R.; Allport, A.; Yang, Q.; Bown, M.; Burns, R.; Maeder, M.; Attalla, M. Carbon Dioxide Postcombustion Capture: A Novel Screening Study of the Carbon Dioxide Absorption Performance of 76 Amines. *Environ. Sci. Technol.* **2009**, *43*, 6427–6433.
- (15) Yeh, J. T.; Resnik, K. P.; Rygle, K.; Pennline, H. W. Semi-Batch Absorption and Regeneration Studies for CO₂ Capture by Aqueous Ammonia. *Fuel Process. Technol.* **2005**, *86*, 1533–1546.
- (16) Yeh, A. C.; Bai, H. Comparison of Ammonia and Monoethanolamine Solvents to Reduce CO₂ Greenhouse Gas Emissions. *Sci. Total Environ.* **1999**, *228*, 121–133.
- (17) Yeh, J. T.; Resnik, K. P.; Pennline, H. W. Regenerable Aqua Ammonia Process for CO₂ Sequestration. *Prepr. Pap. Am. Chem. Soc., Div. Fuel Chem.* **2004**, *49*, 248–249.
- (18) Mani, F.; Peruzzini, M.; Stoppioni, P. CO₂ Absorption by Aqueous NH₃ Solutions: Speciation of Ammonium Carbamate, Bicarbonate and Carbonate by a ¹³C NMR Study. *Green Chem.* **2006**, *9*, 995–1000.
- (19) Loerting, T.; Tautermann, C.; Kroemer, R. T.; Kohl, I.; Hallbrucker, A.; Mayer, E.; Liedl, K. R. Carbonic Acid (H₂CO₃) on the Finger Tip. *Angew. Chem., Int. Ed.* **2000**, *39*, 892–894.
- (20) Tautermann, C.; Voegelé, A. F.; Loerting, T.; Kohl, I.; Hallbrucker, A.; Mayer, E.; Liedl, K. R. Towards the Experimental Decomposition Rate of Carbonic Acid (H₂CO₃) in Aqueous Solution. *Chem.—Eur. J.* **2002**, *8*, 66–73.
- (21) Caplow, M. Kinetics of Carbamate Formation and Breakdown. *J. Am. Chem. Soc.* **1968**, *90*, 6795–6803.
- (22) Danckwerts, P. V. The Reaction of CO₂ with Ethanolamines. *Chem. Eng. Sci.* **1979**, *34*, 443–446.
- (23) Crooks, J. E.; Donnellan, J. P. Kinetics and Mechanism of the Reaction between Carbon Dioxide and Amines in Aqueous Solution. *J. Chem. Soc., Perkin Trans.* **1989**, *2*, 331–333.
- (24) da Silva, E. F.; Svendsen, H. F. Ab Initio Study of the Reaction of Carbamate Formation from CO₂ and Alkanolamines. *Ind. Eng. Chem. Res.* **2004**, *43*, 3413–3418.
- (25) Arstad, B.; Blom, R.; Swang, O. CO₂ Absorption in Aqueous Solutions of Alkanolamines: Mechanistic Insight from Quantum Chemical Calculations. *J. Phys. Chem. A* **2007**, *111*, 1222–1228.
- (26) Baer, T.; Hase, W. L. Unimolecular Reaction Dynamics. *Theory and Experiment*; Oxford University Press: New York, 1996.
- (27) Skodje, T.; Truhlar, D. G. Parabolic Tunneling Calculations. *J. Phys. Chem.* **1981**, *85*, 624–628.
- (28) Foresman, J. B.; Keith, T. A.; Wiberg, K. B.; Snoonian, J.; Frisch, M. J. Solvent Effects. 5. Influence of Cavity Shape, Truncation of Electrostatics, and Electron Correlation on Ab Initio Reaction Field Calculations. *J. Phys. Chem.* **1996**, *100*, 16098–16104.
- (29) Derks, P. W. J.; Versteeg, G. F. Kinetics of Absorption of Carbon Dioxide in Aqueous Ammonia Solutions. *Energy Procedia* **2009**, *1*, 1139–1146.
- (30) Figueroa, J. D.; Fout, T.; Plasynski, S.; McIlvried, H.; Srivastava, R. D. Advances in CO₂ Capture Technology — The U.S. Department of Energy's Carbon Sequestration Program. *Int. J. Greenhouse Gas Control* **2008**, *2*, 9–20.
- (31) Maginn, E. J. What to Do with CO₂. *J. Phys. Chem. Lett.* **2010**, *1*, 3478–3479.